

Celestial Body Surface Mapping for Resource Discovery Using Satellites [†]

Yuxian Li ^{*}, Cesar Vargas-Rosales ^{*ID} and Rafaela Villalpando-Hernandez ^{ID}

Tecnologico de Monterrey, School of Engineering and Sciences, Monterrey 64849, Mexico;
rafaela.villalpando@tec.mx

^{*} Correspondence: a00829851@tec.mx (Y.L.); cvargas@tec.mx (C.V.-R.)

[†] Presented at the 10th International Electronic Conference on Sensors and Applications (ECSA-10), 15–30 November 2023; Available online: <https://ecsa-10.sciforum.net/>.

Abstract: Exploring the solar system provides new possibilities for the survival and development of humankind. Although we do not yet have the technology to migrate on a large scale, we must first find proper celestial bodies, understand their environment, and utilize them. In the future, with highly developed space technology, planets and natural satellites will become “islands” in the solar system for human settlements. However, the lack of information on this matter is one of the greatest challenges in this field. And, for the purpose of geographic data collection, improvements in surface precision and resolution with highly accurate 3D modeling and 2D maps are needed, and the surface of celestial bodies should be mapped by making full use of geometry and different types of map projection methods. Different techniques should be used for the accurate localization of rovers using satellites, thus combining both to create a map of the resource distribution. In this article, a projection method based on conventional techniques for better accuracy and efficiency of mapping and projections of a celestial body is proposed. For further research, hardware enhancements, improvements in multimodal techniques, and the development of communication protocols for rovers and satellites could be pivotal.

Keywords: projection mapping; localization algorithm; surface construction



Citation: Li, Y.; Vargas-Rosales, C.; Villalpando-Hernandez, R. Celestial Body Surface Mapping for Resource Discovery Using Satellites. *Eng. Proc.* **2023**, *58*, 14. <https://doi.org/10.3390/ecsa-10-15998>

Academic Editor: Francisco Falcone

Published: 15 November 2023



Copyright: © 2023 by the authors. Licensee MDPI, Basel, Switzerland. This article is an open access article distributed under the terms and conditions of the Creative Commons Attribution (CC BY) license (<https://creativecommons.org/licenses/by/4.0/>).

1. Introduction

The observation of celestial bodies has evolved with the use of advanced instruments, and their surface projection for resource localization serves as inspiration for humankind. To discover features, projection methods used for the surface of the Earth are used, e.g., the Mercator, Behrmann, and Lambert methods [1]. Yet, they have inefficiencies; e.g., the Mercator method, which is spherically based, is not suitable for elliptical shapes (significant differences far from the Equator) [1].

In this paper, a projection method integrating the characteristics of other methods is proposed to improve accuracy and data collection and to help in the exploration of celestial bodies through a satellite system. Using already existing methods, in cooperation with a rover, a map of the distribution of elements and key features of the celestial body surface is built.

The rest of the paper is organized as follows: in Section 2, the general idea about the proposal is described, and the 2D/3D projection methods are explained. Section 3 gives details about the algorithms for the satellites. Then, the instrument requirements are explained in Section 4. Section 5 is designated for the discussion, and finally, Section 6 for the conclusions.

2. Revolutionizing Celestial Body Projection

Methods to project the surface of the Earth have been used to better understand it. However, all methods have errors due to factors such as gravitational perturbations, atmo-

spheric conditions, and instrument errors, and by combining methods, a new approach with features from all can be obtained. The proposed method is a mixture of other methods, where the projection method uses geometry and satellites jointly to form images and to create 2D/3D maps. Algorithms, jointly with on-surface vehicles, create resource distribution maps. We use the case of Mars; however, this method is valid for similar celestial bodies.

Proposed Method

The method integrates seven low orbit satellites in the exosphere (above 200 km [2]) of Mars, where atmospheric density can be ignored, gravity is almost imperceptible, and low energy consumption is achieved [2] (page 39). The satellite orbit inclination needs to be the same as that of Mars, 25.2°. With equations for motion and dynamic force models acting on the satellite, like atmospheric drag, among others, one can calculate the orbit. Our purpose is not to obtain the orbits, since algorithms already exist [3]. Thus, without a loss of generality, we let the inclination of Mars be 0° (Figure 1A), and by dividing Mars into six parts with similar areas using seven satellites, one oversees the areas of Mars as shown in Figure 1B.

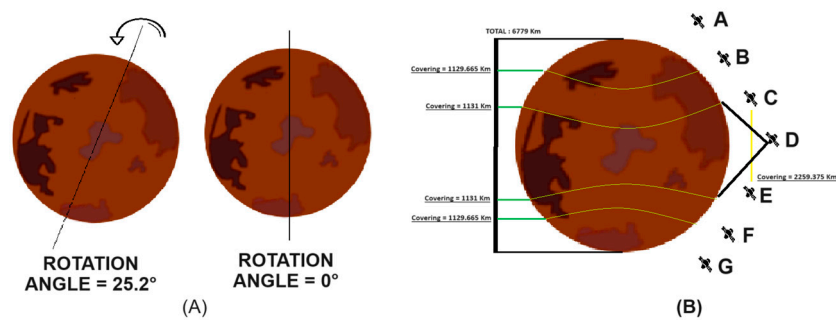


Figure 1. (A) Mars inclination angle. (B) General view of the satellite system where surface coverage is performed by seven satellites identified as A–G.

For satellite A (see Figure 2A), the distance to the surface (altitude $x = 250$ km) is $d = \sqrt{(1129.665 + x)^2 + (1129.665 + x)^2} = 1951.14$ km. Then, it can be located at approximately 1951.14 km at an angle of 45° from the origin of the surface to cover the 1129.665 km radius. Since Mars is spherical, satellite G has the same characteristics as A for the lower part of Mars. For the second area, satellite B has to be placed just at the edge of what satellite A reaches (1129.665 km). Satellites B and C have the same altitude, which defines a straight plane. Satellites are equipped with monitoring cameras, and their angles and the minimum distances they need to reach (the hypotenuse) are obtained using trigonometry, where the opposite and adjacent sides are the longitude and latitude of Mars. For B and F, the camera has a wide angle of 127.874° and a minimum distance of 1432.8194 km for a coverage of 1131 km, i.e., $\sphericalangle = \tan^{-1}(1129.665 - \text{altitude}/1131) = 37.874^\circ + 90^\circ = 127.874^\circ$. Also, for C and E (see Figure 2B), the camera angle is 24.2308° with a minimum distance of 1156.997 km for the coverage, i.e., $\sphericalangle = \tan^{-1}(1131/(2260 + \text{altitude})) = 24.2308^\circ$.

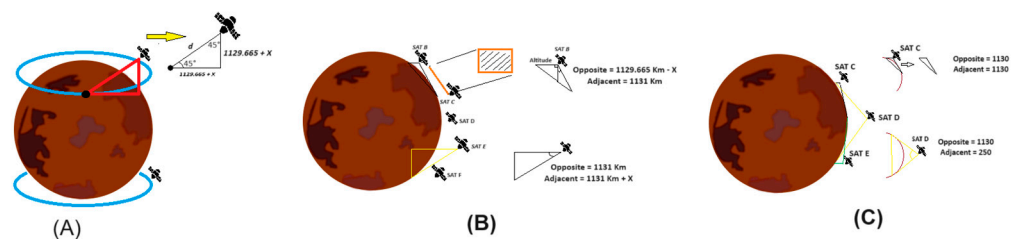


Figure 2. (A) Representation of satellite A and G and orbit trajectory. (B) Projection and coverage for the satellites B, C, E and F. (C) Coverage and the angle of satellite D.

Note that the higher the altitude is, the smaller the angle and the easier it is to adjust the camera position. The Mercator method projects the surface between satellites C and D with the same altitude. The orbit of satellite D forms a cylinder, inside which Mars is located. Satellites C and E will have cameras rotating for the multimodal technique, for better resolution and accuracy. Regarding Figure 2C, we obtain the condition of the camera’s angle as follows: $\angle = \tan^{-1}(1130/altitude) = 77.524^\circ \times 2 = 155.049^\circ$, and the minimum distance satellite D covers (2260 km) is given by $Hypotenuse(SAT D) = 1157.3245 \text{ km}$.

3. Algorithms for Enhancing Surface Condition Capture

With the coverage areas defined, each satellite, except A and G, rotates the camera for the multimodal technique. For satellites A and G, which are within a hexagon (see Figure 3A), there are six points of contact, indicating positions (separated 722.39 km) where images of the surface are taken, i.e., $C = \pi \times 1129.665 + altitude \rightarrow \frac{C}{6} = 722.39\text{km}$. For the remaining satellites, the orbits are divided into 12 points, and a dodecagon is formed (see Figure 3B). Between each point, a rotation of the camera is performed with angles already calculated and pointing directions of camera indicated by the arrows (see Table 1). For satellites B and F, the points are separated $\frac{C}{12} = 361.195\text{km}$. By rotating the camera, satellites A and C take shots with different angles for zones 1 and 2, respectively. For satellites C and E, we have $C = \pi \times 2260 + altitude \rightarrow \frac{C}{12} = 591.666\text{km}$. For satellite D, rotation is not necessary, due to its coverage angle (155.049°).

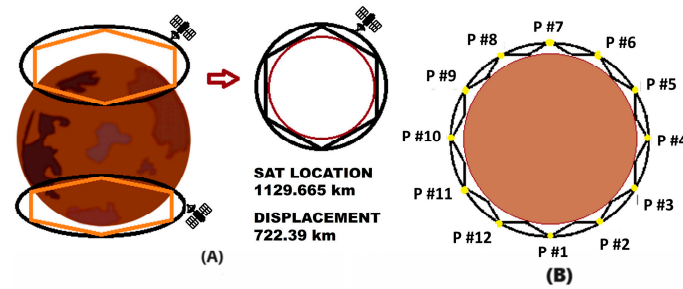


Figure 3. (A) Positions for SAT A and F shots. (B) Dodecagon and points for the remaining satellites.

Table 1. Summary of relationship between taking shots and positions for a single iteration. Arrows indicate up or down direction the camera is pointing at.

Sat/# Position													Distance between Points (km)	Up Angle	Down Angle
SAT A	1↓	2↓	3↓	4↓	5↓	6↓							722.39	None	45°
SAT B	1↑	2↓	3↑	4↓	5↑	6↓	7↑	8↓	9↑	10↓	11↑	12↓	361.195	39.310°	127.874°
SAT C	1↓	2↑	3↓	4↑	5↓	6↑	7↓	8↑	9↓	10↑	11↓	12↑	591.667	39.3165°	127.874°
SAT D	1←	2←	3←	4←	5←	6←	7←	8←	9←	10←	11←	12←	952.687	155.049°	None
SAT E	1↑	2↓	3↑	4↓	5↑	6↓	7↑	8↓	9↑	10↓	11↑	12↓	591.667	127.874°	39.3165°
SAT F	1↓	2↑	3↓	4↑	5↓	6↑	7↓	8↑	9↓	10↑	11↓	12↑	361.195	127.874°	39.3165°
SAT G	1↑	2↑	3↑	4↑	5↑	6↑							722.39	45°	None

The rotation algorithm is summarized in Table 2A. Once the positions are defined, when the system achieves a cycle of its trajectory, a map is generated due to the relatively large distance between points. The benefit of orbits with 6 and 12 points is the assurance that for each orbit, the reference of the system is always the central axis. The seven satellites will always form a straight line, which ensures that the relationship is maintained (see Figure 4) for the various shots of each satellite (see Table 2B).

Table 2. (A) Summary for rotation orders. (B) Distance between points considering 360 points.

SAT/# Point	(A)		(B)	
	Even	Odd	Satellites	<i>N</i>
SAT A	DOWN	DOWN	SAT A	12.0398 km
SAT B	DOWN	UP	SAT B	12.0398 km
SAT C	UP	DOWN	SAT C	21.9038 km
SAT D	CENTER	CENTER	SAT D	31.756 km
SAT E	DOWN	UP	SAT E	12.0398 km
SAT F	UP	DOWN	SAT F	12.0398 km
SAT G	UP	UP	SAT G	12.0398 km

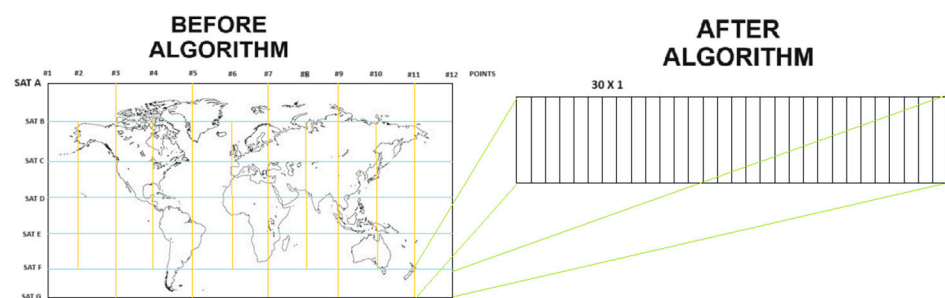


Figure 4. Before and after applying the displacement algorithm.

Displacement Algorithm

To improve the accuracy and observation of Mars’ surface, satellites rotate for the hexagon and dodecagon, with orbits divided into 360 points where satellites are always located. The separation distances of the adjacent points, *N*, are noted in Table 2B. For example, regarding satellite B, after the first iteration (point 1), point 1 + *N* takes place. So, with a displacement of 30 points, point 1 is now point 2. However, the algorithm works in cooperation with the camera rotation, and it is necessary to reach 60 iterations to have at least two shots of a zone. After some iterations, Mars is classified with 360 lines (Figure 4). For A and G, only 30 iterations are needed for 360 lines, since the camera position is always the same.

4. Operation Requirements

The multimodal technique involves having several images of the same area from different angles. This results in a unified image with all the features, improving accuracy in location and aiding in data interpretation; thus, a fusion multimodal data model is proposed [4]. Initially, two images are obtained, but over time, a precise map is created through the combination of a large number of images. The key aspect is that with each iteration of the satellite, the map of the surface becomes clearer and more accurate.

4.1. Location for Rover

High-precision rover positioning is a principal factor for the safety of the rover. In planetary exploration, navigation and positioning, the absence of the Global Positioning System (GPS) and the lack of references are the most complicated parts. Thus, the use of localization algorithms is proposed, such as the SQP algorithm, where two satellites efficiently determine the location of an object [5], or the utilization of Mars rover images of ground rocks and satellite images for rock distribution pattern matching to determine the location [6]. Other techniques can be used, e.g., radio measurement positioning. After positioning and communication with satellites, the process of acquiring data begins. Information such as images of the surface is obtained. The creation of stereoscopic images, 3D

point cloud data, orthophotos, contour maps and slope maps can be obtained based on the collected data, which is useful for subsequent explorations.

4.2. Hardware and Software

The rover requirements, such as the robot arms, antennas, solar panel, Navigation Camera (Navcam), Panoramic Camera (Pancam), and Obstacle Avoidance Camera (Hazcam) [7], are based on the Spirit model. Also, the CheMin Inlet is key, as it is capable of identifying the minerals and chemical composition of rocks and soil [8]. To obtain projections and mapping, this hardware plays an important role with a system with CubeSats. Apart from the hardware that all CubeSats commonly have, e.g., a camera, a power system, and a transmission system [9], some aspects needed to improve efficiency are the following:

- A small, adaptable and stable high-resolution thermal infrared imaging system [10], with a broadband detector array and a compact mechanical cryocooler. The camera includes a sensor chip with a 25 μm pitch and a resolution of 640×512 pixels.
- High spectral resolution cameras installed in the satellites, helping the resource discovery when the rover does not recognize resources or when it is not able to get to some location.
- The rotation system for cameras is necessary to adjust the camera to specific angles for taking photographs. It is based on an odometer and the inertial measurement unit (IMU).
- The inertial measurement unit (IMU) to measure and record acceleration, orientation, angular rates, and gravitational forces. With this, the location or number of points where the satellite is situated can be identified.
- A UHF communication link. This is a necessary transceiver for communication. It can be similar to that used in China's Mars exploration mission, for 'Tianwen One' where the Ultra-High Frequency system was tasked with delivering communication services between the Lander and Encircler during the entry, descent and landing (EDL) phases [11].

With localization and mineral inspection, it is possible to achieve both 2D and 3D mapping of surfaces and mineral distributions. This can be conducted using data collected from the rover and the satellites that are then analyzed with existing software programs such as the following:

- Celestial mapping system (CMS) used for the visualization and analysis of celestial bodies [12]. This application utilizes outdated data from NASA missions. However, we would begin by inputting the gathered information, typically presented in coordinates. As the second step, customization enables the display of specific information. The final step is generating a 2D or 3D map. It is important to note that this process involves updating existing data with new information to generate new maps.
- Nasa's solar system treks, which is a set of tools that provides access to planetary data [13]. First, the desired planet is selected, and as the second step, the different tools are selected to modify the coordinates, visualization, or other features based on the data collected using the proposed method. Ultimately, this software enables us to generate 2D/3D maps for further analysis and allows us to create virtual journeys across the surfaces of planets.

5. Discussion

All projection methods are capable of mapping a celestial body, regardless of its shape, whether spherical or elliptical. However, when compared to other traditional methods, the Berghaus star projection displays distortion mainly in the corners and edges. Also, the polar regions present significant challenges when utilizing the equidistant projection with two points, due to the great distance between the poles. Nevertheless, the proposed projection method is free of distortion, and it has the ability to become increasingly detailed and accurate, depending on the multimodal method and the number of iterations. Furthermore, it is better developed for small celestial bodies, due to limited hardware

capabilities (see Table 3) based on [1]. To enhance accuracy, in addition to requiring more sensors or satellites, it is imperative to establish more shot points for a better resolution. Communication between the satellite and rover is essential, and guiding the rover to the best route for a destination could potentially extend the rover's lifespan. Also, hardware for the spectrometer analysis on the satellite could help identify minerals in areas unreachable for the rover, thereby prolonging the rover's lifespan.

Table 3. Comparison of different projection features.

Projections	Poles Zone Precision	Equator Zone Precision	Limitations	Growth Capacity
Bonne's Equator	Low	Low	Suitable for small-scale maps, and not appropriate for illustrating vast regions	No
Berghaus star	Affected by central point	Affected by central point	Complex mathematical calculations, and not for small zones	No
Two points equidistant	High	Low	Beyond two specific points, shape may lose accuracy in other regions	No
Mercator	Low	High	Unsuitable for representing global maps, due to significant distortion	No
Proposed method	High	High	Limited by hardware design, resolution depends on multimodal technique	Yes

6. Conclusions

The proposed method has extensive potential, as it allows for a time evolution beyond the consideration of several established projection methods. The distinct advantage that it has over other approaches is that it yields a higher number of iterations, which results in more precise surface imaging. However, such precision may ultimately be constrained by hardware limitations, but the problem can be optimized by periodic data transmission processes to Earth for storage and processing. Also, it could be enhanced with hardware upgrades, the implementation of the multimodal technique, and improvements in the communication between the rover and satellites. Similarly, through collaboration with the rover, a successful mineral discovery on the surface can be achieved, followed by marking specific locations on a map for future use. Future research will be focused on enhancing hardware, implementing the multimodal technique, and improving communication methods between the rover and satellites.

Author Contributions: Conceptualization, Y.L. and C.V.-R.; methodology, Y.L.; validation, Y.L. and R.V.-H.; investigation, Y.L.; resources, C.V.-R. and R.V.-H.; writing—original draft preparation, Y.L.; writing—review and editing, C.V.-R. and R.V.-H.; supervision, C.V.-R. and R.V.-H.; project administration, C.V.-R. All authors have read and agreed to the published version of the manuscript.

Funding: This research received no external funding.

Institutional Review Board Statement: Not applicable.

Informed Consent Statement: Not applicable.

Data Availability Statement: Data are contained within the article.

Acknowledgments: We would like to acknowledge the support from the Smart Digital Technologies and Infrastructure Research Group, the project "Digital Technologies to Create Adaptive Smart Cities" of the Challenge-Based Research Program, and the School of Engineering and Science at Tecnológico de Monterrey for providing the means to develop this collaborative work.

Conflicts of Interest: The authors declare no conflict of interest.

References

1. Esri. (s.f.). Mercator Projection. ArcGIS. Available online: <https://desktop.arcgis.com/zh-cn/arcmap/latest/map/projections/mercator.htm> (accessed on 1 September 2023).
2. Haider, S.A. *Aeronomy of Mars*; Springer Nature: Berlin/Heidelberg, Germany, 2023.
3. David, H.; Bohn, P. Precise orbit determination for low earth orbit satellites. *Ann. Marie Curie Fellowsh.* **2006**, *4*, 128–135.

4. Castillo, A.C.; Marroquin-Escobedo, J.A.; Gonzalez-Irigoyen, S.; Martinez-Santoyo, M.; Villalpando-Hernandez, R.; Vargas-Rosales, C. Recreating Lunar Environments by Fusion of Multimodal Data Using Machine Learning Models. *Eng. Proc.* **2022**, *27*, 54. [[CrossRef](#)]
5. Ma, X.; Ning, X.; Chen, X.; Liu, J. Geometric Coplanar Constraints-Aided Autonomous Celestial Navigation for Spacecraft in Deep Space Exploration. *IEEE Access* **2019**, *7*, 112424–112434. [[CrossRef](#)]
6. Kaichang, D.; Zongyu, Y.; Zhaoqin, L. A new method for Mars rover positioning based on the integration of ground images and satellite images. *Spacecr. Eng.* **2010**, *19*, 8–16.
7. NASA FACTS. Mars Exploration Rovers. Available online: https://d2pn8kiwq2w21t.cloudfront.net/documents/mars03rovers_t6lfTK7.pdf (accessed on 10 September 2023).
8. NASA. ChemCam Instrument (Chemistry and Camera). Mars Science Laboratory—Curiosity Rover. Available online: <https://mars.nasa.gov/msl/spacecraft/instruments/chemin> (accessed on 3 September 2023).
9. Sophia, S.; Bott, L.; Fong, A.; Morley, J. Ag2030: AWES-The Cubesat solution. 2022. Available online: https://www.nysf.edu.au/wp-content/uploads/2022/02/1_Innovation-Proposal_Jacinta-Morely-Lucy-Bott-and-Sophia-Seumahu-.pdf (accessed on 10 September 2023).
10. NASA. NASA Technology Transfer Portal. CubeSat Compatible High Resolution Thermal Infrared Imager (GSC-TOPS-138). Available online: <https://technology.nasa.gov/patent/GSC-TOPS-138> (accessed on 5 September 2023).
11. Zezhou, S.; Huiping, Q.; Yu, H.; Fan, B.; Ting, Z.; Ji, X. Design of UHF band relay communication system for “Tianwen-1” Mars probe. *J. Nanjing Univ. Aeronaut. Astronaut./Nanjing Hangkong Hangtian Daxue Xuebao* **2022**, *54*, 5.
12. Celestial Mechanics and Dynamical Astronomy. Available online: <https://celestial.arc.nasa.gov/> (accessed on 10 September 2023).
13. Solar System Treks. Available online: <https://trek.nasa.gov/> (accessed on 10 September 2023).

Disclaimer/Publisher’s Note: The statements, opinions and data contained in all publications are solely those of the individual author(s) and contributor(s) and not of MDPI and/or the editor(s). MDPI and/or the editor(s) disclaim responsibility for any injury to people or property resulting from any ideas, methods, instructions or products referred to in the content.